

Incremental Cluster Validity Indices for Hard Partitions: Extensions and Comparative Study

Leonardo Enzo Brito da Silva, *Member, IEEE*, Niklas M. Melton, *Member, IEEE*,
Donald C. Wunsch II, *Fellow, IEEE*

Abstract

Validation is one of the most important aspects of clustering, but most approaches have been batch methods. Recently, interest has grown in providing incremental alternatives. This paper extends the incremental cluster validity index (iCVI) family to include incremental versions of Calinski-Harabasz (iCH), I index and Pakhira-Bandyopadhyay-Maulik (iI and iPBM), Silhouette (iSIL), Negentropy Increment (iNI), Representative Cross Information Potential (iRCIP) and Representative Cross Entropy (iRH), and Conn_Index (iConn_Index). Additionally, the effect of under- and over-partitioning on the behavior of these six iCVIs, the Partition Separation (PS) index, as well as two other recently developed iCVIs (incremental Xie-Beni (iXB) and incremental Davies-Bouldin (iDB)) was examined through a comparative study. Experimental results using fuzzy adaptive resonance theory (ART)-based clustering methods showed that while evidence of most under-partitioning cases could be inferred from the behaviors of all these iCVIs, over-partitioning was found to be a more challenging scenario indicated only by the iConn_Index. The expansion of incremental validity indices provides significant novel opportunities for assessing and interpreting the results of unsupervised learning.

Index Terms

Clustering, Validation, Incremental Cluster Validity Index (iCVI), Fuzzy, Adaptive Resonance Theory (ART).

L. E. Brito da Silva is with the Applied Computational Intelligence Laboratory, Department of Electrical and Computer Engineering, Missouri University of Science and Technology, Rolla, MO 65409 USA, and also with the CAPES Foundation, Ministry of Education of Brazil, Brasília, DF 70040-020, Brazil (e-mail: leonardoenzo@ieee.org).

N. M. Melton is with the Applied Computational Intelligence Laboratory, Department of Electrical and Computer Engineering, Missouri University of Science and Technology, Rolla, MO 65409 USA (e-mail: niklasmelton@ieee.org).

D. C. Wunsch II is with the Applied Computational Intelligence Laboratory, Department of Electrical and Computer Engineering, Missouri University of Science and Technology, Rolla, MO 65409 USA (e-mail: Wunsch@ieee.org).

I. INTRODUCTION

Cluster validation [1] is a critical topic in cluster analysis. It is crucial to assess the quality of the partitions detected by clustering algorithms when there is no class label information. Different clustering solutions may be found by distinct algorithms, or even by the same algorithm subjected to different hyper-parameters or a different input presentation order [2], [3]. *Cluster validity indices* (CVIs) perform the role of evaluators of such solutions. CVIs typically exhibit a trade-off between measures of compactness (within-cluster scatter) and isolation (between-cluster separation) [2]. Numerous examples of such criteria have been presented in the literature; for comprehensive reviews and experimental studies the interested reader can go to [4]–[11].

Recently, *incremental cluster validity indices* (iCVIs) have been developed to track the effectiveness of online clustering methods over data streams [12]–[15]. To enable cluster validation in such applications, a recursive formulation of compactness was introduced in [12], [13]. This strategy has been used to develop incremental versions of four CVIs so far [15]: viz., incremental Davies-Bouldin (iDB) [12], [13], incremental Xie-Beni (iXB) [12], [13] and modified Dunn’s indices [16]. Particularly, the behavior of iXB and iDB are analyzed in both accurately and poorly partitioned data sets in [12], [13], whereas the studies in [14], [15] only investigate the iDB’s behavior in cases where online clustering algorithms accurately detect data structures, *i.e.*, when they yield high performing experimental results.

Therefore, the contributions of this work are three-fold: (1) presenting incremental versions of six additional CVIs (thereby extending the family of iCVIs), (2) discussing the interpretation of these novel iCVIs in cases of accurately, under- and over-partitioning, and (3) performing a systematic comparative study among ten iCVIs. To explore such scenarios, fuzzy adaptive resonance theory (ART)-based clustering methods [17], [18] were chosen for their simple parameterization of cluster granularity and other appealing properties [19].

The following, Section II, provides a brief review of CVIs, iCVIs and ART; Section III presents this work’s extensions of several other CVIs to the incremental family; Section IV details the set-up used in the numerical experiments; Section V describes and discusses the results; Section VI compares batch and incremental versions of CVIs; and Section VII summarizes this paper’s findings.

II. BACKGROUND AND RELATED WORK

This section briefly recaps the theory regarding the CVIs, iCVIs and ART-based clustering algorithms used in this study.

A. Cluster Validity Indices (CVIs)

Consider a data set $\mathbf{X} = \{\mathbf{x}_i\}_{i=1}^N$ and its hard partition $\Omega = \{\omega_i\}_{i=1}^k$ of k disjointed clusters ω_i , such that $\bigcup_{i=1}^k \omega_i = \mathbf{X}$. In the following CVI overview, \mathbf{v} is a cluster prototype (centroid), k is the number of clusters, d is the dimensionality of the data ($\mathbf{x}_i \in \mathbb{R}^d$), $\|\cdot\|$ is the Euclidean norm, and N and n_i are the cardinalities of a data set and cluster ω_i , respectively.

1) *Calinski-Harabasz (CH)* [20]: the CH index is defined as:

$$CH = \frac{BGSS / (k - 1)}{WGSS / (N - k)}, \quad (1)$$

where the between group sum of squares (BGSS) and within group sum of squares (WGSS) are computed as:

$$WGSS = \sum_{i=1}^k \sum_{\substack{j=1 \\ \mathbf{x}_j \in \omega_i}}^{n_i} \|\mathbf{x}_j - \mathbf{v}_i\|^2, \quad (2)$$

$$BGSS = \sum_{i=1}^k n_i \|\mathbf{v}_i - \boldsymbol{\mu}_{data}\|^2, \quad (3)$$

$$\boldsymbol{\mu}_{data} = \frac{1}{N} \sum_{i=1}^N \mathbf{x}_i. \quad (4)$$

This is an optimization-like criterion [8] such that larger values of CH indicate better clustering solutions (maximization).

2) *Davies-Bouldin (DB)* [21]: the DB index averages the similarities R of each cluster i with respect to its maximally similar cluster $j \neq i$:

$$DB = \frac{1}{k} \sum_{i=1}^k R_i, \quad (5)$$

where

$$R_i = \max_{i \neq j} \left(\frac{S_i + S_j}{M_{i,j}} \right), \quad (6)$$

$$S_l = \left[\frac{1}{n_l} \sum_{\substack{m=1 \\ \mathbf{x}_m \in \omega_l}}^{n_l} \|\mathbf{x}_m - \mathbf{v}_l\|^q \right]^{\frac{1}{q}}, \quad l = \{1, \dots, k\}, \quad (7)$$

$$M_{i,j} = \left[\sum_{t=1}^d |v_{it} - v_{jt}|^p \right]^{\frac{1}{p}}, \quad p \geq 1. \quad (8)$$

The variables (p, q) are user-defined parameters, and S_l and $M_{i,j}$ (Minkowski metric) measure compactness and separation, respectively. Smaller values of DB indicate better clustering solutions (minimization).

3) *Xie-Beni (XB) [22]*: the XB index was originally designed to detect compact and separated clusters in fuzzy c-partitions. A hard partition version is given by the following ratio of compactness to separation [23], [24]:

$$XB = \frac{WGSS/N}{\min_{i \neq j} \|v_i - v_j\|^2}. \quad (9)$$

Smaller values of XB indicate better clustering solutions (minimization).

4) *Pakhira-Bandyopadhyay-Maulik (PBM) [25], [26]*: consider the I index [25] defined as:

$$I = \left(\frac{1}{k} \times \frac{E_1}{E_k} \times D_k \right)^p, \quad p \geq 1, \quad (10)$$

where

$$E_1 = \sum_{i=1}^N \|\mathbf{x}_i - \boldsymbol{\mu}_{data}\|, \quad (11)$$

$$E_k = \sum_{i=1}^k \sum_{\substack{j=1 \\ \mathbf{x}_j \in \omega_i}}^{n_i} \|\mathbf{x}_j - \mathbf{v}_i\|, \quad (12)$$

$$D_k = \max_{i \neq j} (\|\mathbf{v}_i - \mathbf{v}_j\|), \quad (13)$$

The quantities E_k and D_k measure compactness and separation, respectively. This CVI comprises a trade-off among the three competing factors in Eq. (10): $\frac{1}{k}$ decreases with k , whereas both $\frac{E_1}{E_k}$ and D_k increase. By setting $p = 2$ in Eq. (10), the I index reduces to the PBM index [26]. Larger values of PBM indicate better clustering solutions (maximization).

5) *Silhouette (SIL) [27]*: the SIL index is computed by averaging the silhouette coefficients sc_i across all data samples \mathbf{x}_i :

$$SIL = \frac{1}{N} \sum_{i=1}^N sc_i, \quad (14)$$

where

$$sc_i = \frac{b_i - a_i}{\max(a_i, b_i)}, \quad (15)$$

$$a_i = \frac{1}{n_i - 1} \sum_{\substack{j=1, j \neq i \\ \mathbf{x}_j \in \omega_i}}^{n_i} \|\mathbf{x}_j - \mathbf{x}_i\|, \quad (16)$$

$$b_i = \min_{l, l \neq i} \left(\frac{1}{n_l} \sum_{\substack{j=1 \\ \mathbf{x}_j \in \omega_l}}^{n_l} \|\mathbf{x}_j - \mathbf{x}_i\| \right), \quad (17)$$

the variables a_i and b_i measure compactness and separation, respectively. Larger values of SIL (close to 1) indicate better clustering solutions (maximization). To reduce computational complexity, some SIL variants, such as [28]–[31], use a centroid-based approach. The simplified SIL [28], [29] has been successfully used in clustering data streams processed in chunks, in which the silhouette coefficients are also used to make decisions regarding the centroids' incremental updates [32].

6) *Partition Separation (PS)* [33]: the PS index was originally developed for fuzzy clustering; its hard clustering version is given by [34]:

$$PS = \sum_{i=1}^k PS_i, \quad (18)$$

where

$$PS_i = \frac{n_i}{\max_j(n_j)} - \exp \left[-\frac{\min_{i \neq j} (\|\mathbf{v}_i - \mathbf{v}_j\|^2)}{\beta_T} \right], \quad (19)$$

$$\beta_T = \frac{1}{k} \sum_{l=1}^k \|\mathbf{v}_l - \bar{\mathbf{v}}\|^2, \quad (20)$$

$$\bar{\mathbf{v}} = \frac{1}{k} \sum_{l=1}^k \mathbf{v}_l, \quad (21)$$

The PS index only comprises a measure of separation between prototypes. Therefore, this CVI can be readily used to evaluate the partitions identified by unsupervised incremental learners that model clusters using centroids (*e.g.*, [34]). Larger values of PS indicate better clustering solutions (maximization).

7) *Negentropy Increment (NI)* [35], [36]: the NI index measures the average normality of the clusters of a given partition Ω via negentropy [37] while avoiding the direct computation of the clusters' differential entropies. Unlike the other CVIs discussed so far, the NI is not explicitly constructed using measures of compactness and separation [9], [35], thereby being defined as:

$$NI = \frac{1}{2} \sum_{i=1}^k p_i \ln |\Sigma_i| - \frac{1}{2} \ln |\Sigma_{data}| - \sum_{i=1}^k p_i \ln p_i, \quad (22)$$

where $|\cdot|$ denotes the determinant. The probabilities (p), means (\mathbf{v}) and covariance matrices (Σ) are estimated as:

$$p_i = \frac{n_i}{N}, \quad (23)$$

$$\mathbf{v}_i = \frac{1}{n_i} \sum_{\substack{j=1 \\ \mathbf{x}_j \in \omega_i}}^{n_i} \mathbf{x}_j, \quad (24)$$

$$\Sigma_i = \frac{1}{n_i - 1} \sum_{\substack{j=1 \\ \mathbf{x}_j \in \omega_i}}^{n_i} (\mathbf{x}_j - \mathbf{v}_i)(\mathbf{x}_j - \mathbf{v}_i)^T, \quad (25)$$

$$\Sigma_{data} = \frac{1}{N - 1} (\mathbf{X}^T \mathbf{X} - N \boldsymbol{\mu}_{data} \boldsymbol{\mu}_{data}^T), \quad (26)$$

and $\boldsymbol{\mu}_{data}$ is estimated using Eq. (4). Smaller values of NI indicate better clustering solutions (minimization).

8) *Representative Cross Information Potential (rCIP)* [38], [39]: cluster evaluation functions (CEFs) based on cross information potential (CIP) [40], [41] have been consistently used in the literature to evaluate partitions and drive optimization algorithms searching for data structure [38]–[41], thus this work includes these CEFs under the CVI category. Precisely, representative approaches [38], [39] replace the sample-by-sample estimation of Renyi's quadratic Entropy [42] using the Parzen-window method [43] (original CIP [40], [41]) via prototypes and the statistics of their associated Voronoi polyhedron. The rCIP was devised for prototype-based clustering (*i.e.*, two-step methods: vector quantization followed by clustering of the prototypes) [44]–[48]. The CEF used here is defined as [39]:

$$CEF = \sum_{i=1}^{k-1} \sum_{j=i+1}^k rCIP(\omega_i, \omega_j), \quad (27)$$

where

$$rCIP(\omega_i, \omega_j) = \frac{1}{M_i M_j} \sum_{l=1}^{M_i} \sum_{m=1}^{M_j} G(\mathbf{v}_l - \mathbf{v}_m, \Sigma_{l,m}), \quad (28)$$

$$G(\mathbf{v}_l - \mathbf{v}_m, \Sigma_{l,m}) = \frac{e^{-\frac{1}{2}(\mathbf{v}_l - \mathbf{v}_m)^T \Sigma_{l,m}^{-1} (\mathbf{v}_l - \mathbf{v}_m)}}{\sqrt{(2\pi)^d |\Sigma_{l,m}|}}, \quad (29)$$

$\Sigma_{l,m} = \Sigma_l + \Sigma_m$, $\{\mathbf{v}_l, \Sigma_l\} \in \omega_i$, $\{\mathbf{v}_m, \Sigma_m\} \in \omega_j$, M_i and M_j are the number of prototypes used to represent clusters ω_i and ω_j , respectively. The prototypes and covariance matrices are estimated using Eqs. (24) and (25), respectively. Smaller values of CEF indicate better clustering solutions (minimization). Recently, the information potential (IP) [49] measure has been used to define a system's state when modeling and analyzing dynamic processes [50], [51].

9) *Conn_Index* [52], [53]: the *Conn_Index* was also developed for prototype-based clustering. It is formulated using the connectivity strength matrix (*CONN*), which is a symmetric square similarity matrix that represents local data densities between neighboring prototypes [54], [55]. Its $(i, j)^{th}$ entry is formally given by:

$$CONN(i, j) = CADJ(i, j) + CADJ(j, i), \quad (30)$$

where the $(i, j)^{th}$ entry of the non-symmetric cumulative adjacency matrix (*CADJ*) corresponds to the number of samples for which \mathbf{v}_i and \mathbf{v}_j are, simultaneously, the first and second closest prototypes (according to some measure), respectively. The *Conn_Index* is defined as:

$$Conn_Index = Intra_Conn \times (1 - Inter_Conn), \quad (31)$$

where the intra-cluster (*Intra_Conn*) and inter-cluster (*Inter_Conn*) connectivities are:

$$Intra_Conn = \frac{1}{k} \sum_{l=1}^k Intra_Conn(\omega_l), \quad (32)$$

$$Intra_Conn(\omega_l) = \frac{1}{n_l} \sum_{\substack{i,j \\ \mathbf{v}_i, \mathbf{v}_j \in \omega_l}} CADJ(i, j), \quad (33)$$

$$Inter_Conn = \frac{1}{k} \sum_{l=1}^k \max_{\substack{m \\ m \neq l}} [Inter_Conn(\omega_l, \omega_m)], \quad (34)$$

$$Inter_Conn(\omega_l, \omega_m) = \frac{\sum_{\substack{i,j \\ \mathbf{v}_i \in \omega_l, \mathbf{v}_j \in \omega_m}} CADJ(i, j)}{\sum_{\substack{i,j \\ \mathbf{v}_i \in V_{l,m}}} CADJ(i, j)}, \quad (35)$$

$$V_{l,m} = \{\mathbf{v}_i : \mathbf{v}_i \in \omega_l, \exists \mathbf{v}_j \in \omega_m : CADJ(i, j) > 0\}, \quad (36)$$

the variable P is the total number of prototypes, and $Inter_Conn(\omega_l, \omega_m) = 0$ if $V_{l,m} = \{\emptyset\}$. Naturally, the quantities *Intra_Conn* and *Inter_Conn* measure compactness and separation, respectively. Larger values of the *Conn_Index* (close to 1) indicate better clustering solutions (maximization).

B. Incremental Cluster Validity Indices (iCVIs)

The compactness and separation terms commonly found in CVIs are generally computed using data samples and prototypes, respectively [12], [14]. In order to handle online clustering applications demands (*i.e.*, data streams), an incremental CVI (iCVI) formulation that recursively estimates the compactness term was introduced in [12], [13] in the context of fuzzy clustering.

Specifically, consider the hard clustering version of cluster i 's compactness CP (*i.e.*, by setting the fuzzy memberships in [12], [13] to binary indicator functions):

$$CP_i = \sum_{\substack{j=1 \\ \mathbf{x}_j \in \omega_i}}^{n_i} \|\mathbf{x}_j - \mathbf{v}_i\|^2, \quad (37)$$

in such a case, when a new sample \mathbf{x} is presented and encoded by cluster i , then its new compactness becomes:

$$CP_i^{new} = \sum_{\substack{j=1 \\ \mathbf{x}_j \in \omega_i}}^{n_i^{new}} \|\mathbf{x}_j - \mathbf{v}_i^{new}\|^2, \quad (38)$$

where

$$n_i^{new} = n_i^{old} + 1, \quad (39)$$

$$\mathbf{v}_i^{new} = \mathbf{v}_i^{old} + (\mathbf{x} - \mathbf{v}_i^{old})/n_i^{new}, \quad (40)$$

and

$$N^{new} = N^{old} + 1. \quad (41)$$

The compactness in Eq. (38) can be updated incrementally as [12], [13]:

$$CP_i^{new} = CP_i^{old} + \|\mathbf{z}_i\|^2 + n_i^{old} \|\Delta \mathbf{v}_i\|^2 + 2\Delta \mathbf{v}_i^T \mathbf{g}_i^{old}, \quad (42)$$

where

$$\mathbf{g}_i^{new} = \mathbf{g}_i^{old} + \mathbf{z}_i + n_i^{old} \Delta \mathbf{v}_i, \quad (43)$$

$$\mathbf{g}_i = \sum_{j=1}^{n_i} (\mathbf{x}_j - \mathbf{v}_i), \quad (44)$$

$$\mathbf{z}_i = \mathbf{x} - \mathbf{v}_i^{new}, \quad (45)$$

$$\Delta \mathbf{v}_i = \mathbf{v}_i^{old} - \mathbf{v}_i^{new}. \quad (46)$$

The compactness CP and vector \mathbf{g} are initialized as 0 and $\vec{\mathbf{0}}$ (since $\mathbf{v} = \mathbf{x}$), respectively. Note that, at each iteration, the variable \mathbf{g} is updated after CP . Using such incremental formulation, the following iCVIs were derived in [12], [13] (their hard partition counterparts are shown here)

1) *incremental Xie-Beni (iXB)*:

$$XB^{new} = \frac{1}{N^{new}} \times \frac{\sum_{i=1}^{k^{new}} CP_i^{new}}{\min_{i \neq j} (\|\mathbf{v}_i^{new} - \mathbf{v}_j^{new}\|^2)}, \quad (47)$$

2) *incremental Davies-Bouldin (iDB - based on [56])*:

$$DB^{new} = \frac{1}{k^{new}} \sum_{i=1}^{k^{new}} \max_{j, j \neq i} \left(\frac{\frac{CP_i^{new}}{n_i^{new}} + \frac{CP_j^{new}}{n_j^{new}}}{\|\mathbf{v}_i^{new} - \mathbf{v}_j^{new}\|^2} \right). \quad (48)$$

If a new cluster emerges, then $k^{new} = k^{old} + 1$; otherwise its previous value is maintained. Note that only one prototype \mathbf{v} is updated after each input presentation.

C. Adaptive Resonance Theory (ART)

For this study's experiments, adaptive resonance theory (ART) [57] has been implemented. It is a fast and stable online clustering method with automatic category recognition encompassing a rich history with many implementations well-suited to iCVI computation [17]–[19], [57]–[72]. The following ART models were used in these experiments.

1) *Fuzzy ART [17]*: This model implements fuzzy logic [73] to bound data within hyper-boxes. For a normalized data set $\mathbf{X} = \{\mathbf{x}_i\}_{i=1}^N$ ($0 \leq x_{i,j} \leq 1$, $j = \{1, \dots, d\}$), the fuzzy ART algorithm, with parameters (α, β, ρ) , is defined by:

$$\mathbf{I} = (\mathbf{x}_i, 1 - \mathbf{x}_i), \quad (49)$$

$$T_j = \frac{\|\min(\mathbf{I}, \mathbf{w}_j)\|_1}{\alpha + \|\mathbf{w}_j\|_1}, \quad (50)$$

$$\|\min(\mathbf{I}, \mathbf{w}_j)\|_1 \geq \rho \|\mathbf{I}\|_1, \quad (51)$$

$$\mathbf{w}_j^{new} = \mathbf{w}_j^{old}(1 - \beta) + \beta \min(\mathbf{I}, \mathbf{w}_j^{old}). \quad (52)$$

Equation (49) is the complement coding function, which concatenates sample \mathbf{x} and its complement to form an input vector \mathbf{I} with dimension $2d$. Equation (50) is the activation function for each category j , where $\|\cdot\|_1$ is the L_1 norm, $\min(\cdot)$ is performed component-wise, and α is a tie breaking constant. Each category is checked for validity against Eq. (51)'s vigilance parameter ρ in a descending order of activation. If no valid category is found during training, then a new category is initialized using \mathbf{I} as the new weight vector \mathbf{w} . Otherwise, the winning category is updated according to Eq. (52) using learning rate β . In this study, when fuzzy ART is set to evaluation mode (learning is disabled), if no valid category is found during search, then the winning category defaults to the highest activated one.

2) *Fuzzy self-consistent modular ART (SMART) [18]*: This model is a hierarchical clustering technique based on the ARTMAP architecture [17]. In an ARTMAP network, two ART modules, A- and B-side, are supplied with separate but dependent data streams. Both ART modules can cluster according to local topology and parameters while an inter-ART module enforces a surjective mapping of the A-side to the B-side, effectively learning the functional map of the A-side to the B-side categories.

To build a fuzzy SMART module, it is only necessary to stream the same sample to both the A- and B-sides of a fuzzy ARTMAP module, *i.e.*, use fuzzy ARTMAP in an auto-associative mode. If all else is equal in the A and B modules' parameters, fuzzy SMART will begin to form a two-level self-consistent cluster hierarchy when $\rho_A > \rho_B$. This hierarchy will be required to extend the iCVI study to prototype-based CVIs such as the Conn_Index. For such CVIs, the A-side categories act as cluster prototypes while the B-side provides the actual data partition.

III. EXTENSIONS OF ICVIS

To compute the CVIs mentioned in Section II-A incrementally, employing one of the following approaches is sufficient:

- 1) The recursive computation of compactness developed in [12], [13] (CVIs: CH, I/PBM, and SIL).
- 2) The incremental computation of probabilities, means and covariance matrices (CVIs: rCIP and NI). Naturally, if the clustering algorithm of choice already models the clusters using a priori probabilities, means and covariance matrices (such as Gaussian ART [65] and Bayesian ART [68]), then, similarly to PS, these CVIs can be readily computed.
- 3) The incremental building of a multi-prototype representation of clusters in a self-consistent two-level hierarchy while tracking the density-based connections between neighboring prototypes (CVI: Conn_index). Specifically, increment and/or expand the CADJ and CONN matrices as clusters grow and/or are dynamically created.

In the following iCVIs' extensions (iCH, iI/PBM, iSIL, irCIP, iNI, and iConn_index), if a new cluster is formed after sample \mathbf{x} is presented, then the number of clusters is $k^{new} = k^{old} + 1$, the number of samples encoded by this cluster is $n_{k^{new}}^{new} = 1$, the clusters' prototype is set to $\mathbf{v}_{k^{new}}^{new} = \mathbf{x}$, the initial compactness is $CP_{k^{new}}^{new} = 0$, and vector $\mathbf{g}_{k^{new}}^{new} = \vec{0}$ (unless otherwise noted). Naturally, clusters that do not encode the presented sample remain with constant parameter values for the duration of that input presentation. Also note that, when necessary, the Euclidean

norm is replaced with the squared Euclidean norm (*i.e.*, $\|\cdot\|^2$) to allow for the computation of compactness CP (as per [12], [13]). Finally, for iCVIs that require the computation of pairwise (dis)similarity between prototypes, the (dis)similarity matrix is kept in memory, where only the rows and columns corresponding to the prototype that is adapted are modified.

A. Incremental Calinski-Harabasz index (iCH)

The iCH computation is defined as:

$$CH^{new} = \frac{\sum_{i=1}^{k^{new}} SEP_i^{new}}{\sum_{i=1}^{k^{new}} CP_i^{new}} \times \frac{N^{new} - k^{new}}{k^{new} - 1}, \quad (53)$$

where

$$SEP_i^{new} = n_i^{new} \|\mathbf{v}_i^{new} - \boldsymbol{\mu}_{data}^{new}\|^2. \quad (54)$$

Note that the variables $\{n_1, \dots, n_k\}$, $\{\mathbf{v}_1, \dots, \mathbf{v}_k\}$, $\{CP_1, \dots, CP_k\}$, $\{\mathbf{g}_1, \dots, \mathbf{g}_k\}$, $\boldsymbol{\mu}_{data}$, k , N , and $\{SEP_1, \dots, SEP_k\}$ are all kept in memory. These are updated using Eqs. (39) to (43), except for SEP , which is adapted using Eq. (54). The data mean $\boldsymbol{\mu}_{data}$ is updated similarly to the prototypes \mathbf{v} (*i.e.*, Eq. (40)).

B. Incremental I index (iI)

The iI computation is defined as:

$$I^{new} = \left[\frac{\max_{i \neq j} (\|\mathbf{v}_i^{new} - \mathbf{v}_j^{new}\|^2)}{\sum_{i=1}^k CP_i^{new}} \times \frac{CP_0^{new}}{k^{new}} \right]^p, \quad (55)$$

where CP_0 and $\sum_{i=1}^k CP_i^{new}$ correspond to E_1 and E_k , respectively. These are updated according to Eqs. (39) to (43) along with the remaining compactness variables. Only the pairwise distances with respect to the updated prototype at any given iteration need to be recomputed.

C. Incremental Silhouette index (iSIL)

The SIL index is inherently batch (offline), since it requires the entire data set to be computed (the silhouette coefficients are averaged across all data samples in Eq. (14)). To remove such a requirement and enable incremental updates, a hard version of the centroid-based SIL variant

introduced in [30] is employed here as well as the squared Euclidean norm (*i.e.*, $\|\cdot\|^2$): this is done in order to employ the recurrent formulation of the compactness in Eq. (42). Consider the matrix $\mathbf{S}_{k \times k}$, where k prototypes \mathbf{v}_i are used to compute the centroid-based SIL (instead of the N samples \mathbf{x}_i - which, by definition, are discarded after each presentation in online mode). Define each entry $s_{i,j} = D(\mathbf{v}_i, \omega_j)$ (dissimilarity of \mathbf{v}_i to cluster ω_j) of $\mathbf{S}_{k \times k}$ as:

$$s_{i,j} = \frac{1}{n_j} \sum_{\substack{l=1 \\ \mathbf{x}_l \in \omega_j}}^{n_j} \|\mathbf{x}_l - \mathbf{v}_i\|^2 = \frac{1}{n_j} CP(\mathbf{v}_i, \omega_j), \quad (56)$$

where $i = \{1, \dots, k\}$ and $j = \{1, \dots, k\}$. The silhouette coefficients can be obtained from the entries of $\mathbf{S}_{k \times k}$ as:

$$sc_i = \frac{\min_{l, l \neq J} (s_{i,l}) - s_{i,J}}{\max \left[s_{i,J}, \min_{l, l \neq J} (s_{i,l}) \right]}, \mathbf{v}_i \in \omega_J. \quad (57)$$

where $a_i = s_{i,J}$ and $b_i = \min_{l, l \neq J} (s_{i,l})$.

At first, when examining Eq. (56), one might be tempted to store a $k \times k$ matrix of compactness entries along with their accompanying k^2 vectors \mathbf{g} (one for each entry) to enable incremental updates of each element of matrix of $\mathbf{S}_{k \times k}$; this approach, however, may lead to unnecessarily large memory requirements. A more careful exam shows that it is sufficient to simply redefine CP and \mathbf{g} for each cluster i ($i = \{1, \dots, k\}$) as:

$$CP_i = \sum_{\substack{j=1 \\ \mathbf{x}_j \in \omega_i}}^{n_i} \|\mathbf{x}_j - \vec{\mathbf{0}}\|^2 = \sum_{\substack{j=1 \\ \mathbf{x}_j \in \omega_i}}^{n_i} \|\mathbf{x}_j\|^2, \quad (58)$$

$$\mathbf{g}_i = \sum_{\substack{j=1 \\ \mathbf{x}_j \in \omega_i}}^{n_i} (\mathbf{x}_j - \vec{\mathbf{0}}) = \sum_{\substack{j=1 \\ \mathbf{x}_j \in \omega_i}}^{n_i} \mathbf{x}_j, \quad (59)$$

which is equivalent to fixing $\mathbf{v} = \vec{\mathbf{0}}$. Therefore, their incremental update equations become (as opposed to Eqs. (42) and (43)):

$$CP_i^{new} = CP_i^{old} + \|\mathbf{x}\|^2, \quad (60)$$

$$\mathbf{g}_i^{new} = \mathbf{g}_i^{old} + \mathbf{x}. \quad (61)$$

Using this trick, when a sample \mathbf{x} is assigned to cluster ω_J , then the update equations for each entry $s_{i,j}$ of $\mathbf{S}_{k \times k}$ are given by Eq. (62). Note that the numerators of the expressions in Eq. (62) update the compactness “as if” the prototype has changed from $\vec{\mathbf{0}}$ to \mathbf{v}^{new} at every iteration ($\Delta \mathbf{v} = -\mathbf{v}^{new}$). The remaining variables such as n , N , and \mathbf{v} are updated as previously

described. This allows $\{CP_1, \dots, CP_k\}$ and $\{\mathbf{g}_1, \dots, \mathbf{g}_k\}$ to continue being stored similarly to the previous iCVIs, instead of a $k \times k$ matrix of compactness and the associated k^2 vectors \mathbf{g} .

$$s_{i,j}^{new} = \begin{cases} \frac{1}{n_j^{new}} \left(CP_j^{old} + \|\mathbf{z}_i\|^2 + n_j^{old} \|\mathbf{v}_i^{old}\|^2 - 2\mathbf{v}_i^{old T} \mathbf{g}_j^{old} \right) & , (i \neq J, j = J) \\ \frac{1}{n_j^{old}} \left(CP_j^{old} + n_j^{old} \|\mathbf{v}_i^{new}\|^2 - 2\mathbf{v}_i^{new T} \mathbf{g}_j^{old} \right) & , (i = J, j \neq J) \\ \frac{1}{n_j^{new}} \left(CP_j^{old} + \|\mathbf{z}_j\|^2 + n_j^{old} \|\mathbf{v}_j^{new}\|^2 - 2\mathbf{v}_j^{new T} \mathbf{g}_j^{old} \right) & , (i = J, j = J) \\ s_{i,j}^{old} & , (i \neq J, j \neq J) \end{cases} \quad (62)$$

In the case where a new cluster ω_{k+1} is created following the presentation of sample \mathbf{x} , then a new column and a new row are appended to the matrix $\mathbf{S}_{k \times k}$. Unlike the other iCVIs, the compactness CP_{k+1} and vector \mathbf{g}_{k+1} of this cluster are initialized as $\|\mathbf{x}\|^2$ and \mathbf{x} , respectively. Then, the entries of $\mathbf{S}_{k \times k}$ are updated using Eq. (63).

$$s_{i,j}^{new} = \begin{cases} CP_{k+1} + \|\mathbf{v}_i^{old}\|^2 - 2\mathbf{v}_i^{old T} \mathbf{g}_{k+1} & , (i \neq k+1, j = k+1) \\ \frac{1}{n_j^{old}} \left(CP_j^{old} + n_j^{old} \|\mathbf{v}_i^{new}\|^2 - 2\mathbf{v}_i^{new T} \mathbf{g}_j^{old} \right) & , (i = k+1, j \neq k+1) \\ 0 & , (i = k+1, j = k+1) \\ s_{i,j}^{old} & , (i \neq k+1, j \neq k+1) \end{cases} \quad (63)$$

Following the incremental updates of the entries of $\mathbf{S}_{k \times k}$ (Eq. (62) or (63)), the silhouette coefficients (sc_i) are computed (Eq. (57)), and the iSIL is updated as:

$$SIL^{new} = \frac{1}{k^{new}} \sum_{i=1}^{k^{new}} sc_i^{new}. \quad (64)$$

D. Incremental Negentropy Increment (iNI)

The iNI computation is defined as:

$$NI^{new} = \sum_{i=1}^k p_i^{new} \ln \left(\frac{\sqrt{|\Sigma_i^{new}|}}{p_i^{new}} \right) - \frac{1}{2} \ln |\Sigma_{data}| \quad (65)$$

where $p_i^{new} = n_i^{new} / N^{new}$, and Σ_i^{new} is computed using the following recursive formula [43]:

$$\Sigma^{new} = \frac{n^{new} - 2}{n^{new} - 1} (\Sigma^{old} - \delta I) + \frac{1}{n^{new}} (\mathbf{x} - \mathbf{v}^{old}) (\mathbf{x} - \mathbf{v}^{old})^T + \delta I \quad (66)$$

This work's authors set $\delta = 10^{-\frac{\epsilon}{d}}$ to avoid numerical errors, where ϵ is a user-defined parameter. If a new cluster is created, then $\Sigma = \delta I$ and $|\Sigma| = 10^{-\epsilon}$.

E. Incremental representative Cross Information Potential (*irCIP*) and cross-entropy (*irH*)

Section V will show that using the representative cross-entropy *rH* for computing the CEF makes it easier to observe the behavior of the incremental clustering process (this corroborates a previous study in which *rH* was deemed more informative than *rCIP* for multivariate data visualization [74]):

$$rH(\omega_i, \omega_j) = -\ln[rCIP(\omega_i, \omega_j)], \quad (67)$$

$$CEF = \sum_{i=1}^{k-1} \sum_{j=i+1}^k rH(\omega_i, \omega_j). \quad (68)$$

Note that, as opposed to the *rCIP*-based CEF, larger values of *rH*-based CEF indicate better clustering solutions (maximization). Concretely, since the CEF only measures separation, then, like *iNI*, it is only necessary to update the means and the covariance matrices online in order to construct the incremental CEF (*iCEF*). This is also done using Eqs. (40) and (66), respectively. The *iCEFs*, based on *rCIP* and *rH*, are hereafter referred to as *irCIP* and *irH*, respectively.

F. Incremental Conn_Index (*iConn_Index*)

The *Conn_Index* is another inherently batch CVI, as each element (i, j) of the *CADJ* matrix requires the count of the samples in the data set with the first and second closest prototypes, v_i and v_j respectively. Naturally, when clustering data online, v_i and v_j may change for previously presented samples as prototypes are continuously modified or created. However, for the purpose of building and incrementing *CADJ* and *CONN* matrices online (with only one element changing per sample presentation), it is assumed that the trends exhibited over time by the *iConn_Index* does not differ dramatically from its offline counterpart. Batch calculation can be eliminated entirely by keeping the values of Eqs. (33) and (35) in memory and updating only the entries corresponding to the winning prototype v_i .

In this study, the self-consistent hierarchy and multi-prototype cluster representation required by the *iConn_Index* was generated using fuzzy SMART, whose modules A and B are used for prototype and cluster definition, respectively. Fuzzy SMART's module A was modified in such a way that it forcefully creates two prototypes from the first two samples of every emerging cluster in module B. By enforcing this dynamic, each cluster always possesses at least two prototypes for the computation of the *iConn_Index*. This strategy addresses two problems: first, it allows *CADJ* to be created from the second sample seen and onward; second, it prevents some cases

in which well-separated clusters are strongly connected simply because one of them does not have another prototype to assume the role of the second winner. The second winning prototype for a sample v_j is the winning A-side category when the first winning prototype v_i has been removed from the A-side category set.

The `iConn_Index` demands certain boundary conditions. In the case of exactly one prototype and one category, such as the case for the very first sample presentation, the `CADJ` matrix cannot be incremented, and the `iConn_Index` will default to 0 [53]. This paper presents a remedy for this whereby a count of samples is kept separate from the `CADJ` matrix (instance counting [75]). Upon creation of the second prototype v_2 in fuzzy SMART's module A, the `CADJ` matrix will be incremented for the first time at element (2, 1). At this point, the element (1, 2) will be set to the number of samples seen so far belonging to v_1 . This situation is encountered in the very first sample presentation to fuzzy SMART.

Note that, in the case of a single category, *Inter_Conn*, given by Eq. (34), defaults to 1 [53]. In the case of a category with a single prototype, the *Intra_Conn* for that category, given by Eq. (33), also defaults to a value of 1 [53]. Finally, instead of the original constraint $CADJ(i, j) > 0$ imposed by Eq. (36), this paper's `iConn_Index` implementation uses $CONN(i, j) > 0$, as this makes its behavior smoother and more consistent in this application domain.

IV. NUMERICAL EXPERIMENTS SETUP

The numerical experiments were carried out using the MATLAB software environment. The Cluster Validity Analysis Platform Toolbox [76] was used to compute the Adjusted Rand Index (*ARI*) [77] to evaluate the partitions detected by the fuzzy ART-based clustering algorithms. Two synthetic data sets were used: (1) *R15* [78], [79], consisting of 800 samples and 15 clusters in two dimensions and (2) *D4*, which is an in-house artificially generated data set with 2000 samples and 4 clusters also in two dimensions. For comparison purposes, hard clustering versions of *iDB*, *iXB* and *PS CVIs* were used in the experiments. Finally, it should be noted that this study does not employ multi-prototype representations for the *irCIP* and *irH* (*i.e.*, $M_i = M_j = 1, \forall i, j$ in Eq. (28)) since each of the clusters from the data sets used in these experiments can be modeled using single Gaussian distributions.

All fuzzy ART and SMART dynamics were performed with normalized and complement coded input, whereas the CVI computations were performed using the normalized data. To

emulate scenarios in which there is a natural order of presentation, the samples were presented to fuzzy ART/SMART in a cluster-by-cluster fashion where samples within a given cluster were randomized. Finally, in these experiments, $\epsilon = 12$ in Eq. (66) for the incremental computation of the covariance matrices used by irCIP, irH and iNI. The source code of the CVIs/iCVIs, fuzzy ART/SMART, and experiments is provided at the Applied Computational Intelligence Laboratory public GitLab repository¹.

V. A COMPARATIVE STUDY

This section discusses the behavior of the iCVIs in three general cases when assessing the quality of the partitions detected by fuzzy ART-based systems in real-time: (1) high-quality partitions, (2) under-partitions, and (3) over-partitions. It should be emphasized that this analysis is not focused on evaluating the performance or capabilities of the chosen clustering algorithms, but instead the purpose of this study is to observe the behavior of the iCVIs in these different scenarios to gain insight on their applicability. Moreover, in each of these scenarios, the iCVIs' dynamics are investigated in two sub-cases: (a) the creation of a new cluster and (b) the presentation of samples within a given cluster.

The following discussion is relative to the data sets used in the experiments and their respective order of cluster and sample presentation (Fig. 1). This is not an exhaustive study of all possible permutations of clusters and samples, as each of them may trigger different global behaviors of the iCVIs. Nonetheless, it can be assumed that some behaviors are typical, which allows the inference of some particular problems that may arise during incremental unsupervised learning.

Similar to [12]–[16], a natural ordering, *i.e.*, meaningful temporal information is assumed. The *R15* data set was used to illustrate the behavior of the iCVIs in cases (1) and (2), which are depicted in Figs. 2 and 3, respectively. Alternately, the *D4* data set was used to illustrate the behavior of the iCVIs in cases (1) and (3), which are depicted in Figs. 4 and 5, respectively. For both data sets, case (1) is used as a reference to which their respective cases (2) and (3) are compared. Moreover, Figs. 2 to 5 depict the iCVIs immediately following the creation of the second cluster.

¹<https://github.com/ACIL-Group/iCVIs>

A. Correct estimation and underestimation of the number of clusters

Consider the high-quality partition of the *R15* data set shown in Fig. 2a, which was obtained when presenting samples in the cluster-by-cluster ordering depicted in Fig. 1a. This study shows, in general (and as expected from previous studies on iDB and iXB [12]–[16]), that the drastic changes in most iCVI values follow the emergence of new clusters. The exceptions are the iXB and irCIP, which appear much less informative than the other iCVIs used in this particular experiment, as they show no clearly defined tendencies and seem insensitive to the well-separated clusters numbered 12 to 15 in Fig. 2a.

During the presentation of samples within a given cluster, many different behaviors can be observed. Typically, iCH either improves or has small fluctuations; iSIL and iDB either worsen or have small fluctuations; iI/iPBM and iNI either worsen or improve; iConn_Index and PS improve; and irH consistently undergoes small fluctuations. Again, irCIP and iXB do not appear to be particularly useful compared to the other iCVIs since no apparent trends were found over the iterations. If an iCVI displays more than one trend, these usually do not occur prominently and simultaneously (*i.e.*, during the presentation of samples from the same cluster). Note that these are important characteristics, since they will help in identifying the under-partition cases.

Now consider the case of underestimating the number of clusters, as shown in Fig. 3a. The latter was obtained when presenting samples in the cluster-by-cluster ordering depicted in Fig. 1b. This research notes that most iCVIs consistently worsen while the algorithm incorrectly agglomerates samples from different clusters (clusters numbered 2 to 9 in Fig. 1b) into a single cluster (cluster numbered 2 in Fig. 3a), except for the iConn_Index (which actually improves

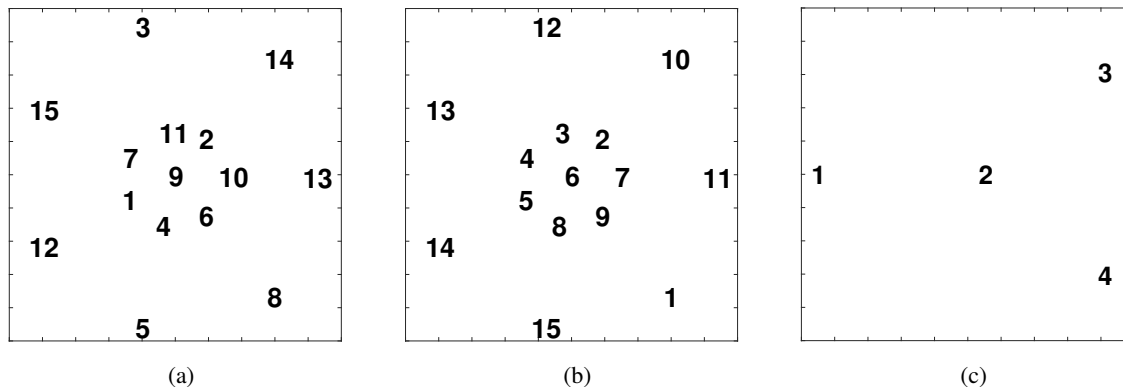


Fig. 1. Presentation order of the classes for the experiments carried out in (a) Fig. 2, (b) Fig. 3, and (c) Figs. 4 and 5.

due to the strong connectivity among prototypes) and irCIP (which remains constant). Moreover, when incorrectly merging clusters 10 and 11 in Fig. 1b into a single cluster labeled 3 in Fig. 3a, the performances of all iCVIs are accompanied by a drastic change typically toward worse values (except for PS, which only undergoes a slight slope change), while the number of clusters remains constant.

The behavior previously described can also be observed for clusters labeled 4 and 1 in Fig. 3a. Drastic (iSIL, irCIP, irH, iNI, iDB, iXB, and iConn_Index) or more subtle (iCH, il/iPBM) changes entailing worsening trends take place in the behavior of all CVIs in Fig. 3 when these samples are classified to the same cluster - again, with the exception of PS, which still improves, but with a different inclination. These clearly indicate that the clustering algorithm is mistakenly encoding the samples under the same cluster umbrella.

At this stage, it is important to be cautious because even when a high-quality partition is retrieved (Fig. 2), some iCVIs (such as iSIL, iConn_Index, and iDB), can both improve and worsen when fuzzy ART is allocating samples to the same cluster (although this happens less frequently and less drastically). Therefore, it is recommended to observe more than one iCVI to determine if under-partition is taking place.

B. Correct estimation and overestimation of the number of clusters

For the sake of clarity, over-partition is illustrated using the *D4* data set, which has a smaller number of clusters. First, the iCVI behaviors regarding the high-quality partition shown in Fig. 4a are observed as a reference; these were obtained using the cluster sequence depicted in Fig. 1c. The same iCVI trends seem to hold following the emergence of new clusters as well as during the presentation of samples belonging to a given cluster (and again, iXB and irCIP provided the least visually descriptive behavior over time). A notable exception, however, is the iNI, which quickly improves immediately after the creation of a new cluster and then worsens as samples from the same cluster are presented. This supports the fact that the iCVI behaviors are not universal: naturally, they are data- and order-dependent.

Now consider the over-partition problem depicted in Fig. 5a, which was also obtained using the cluster sequence depicted in Fig. 1c. As expected, a steep descent (or ascent depending on the iCVI) usually occurs when new clusters are created. However, since this trend appears to occur regardless of the partition quality (being inherent to all iCVIs), then it is not sufficient to identify this issue. In this scenario, unless there was additional a priori information (*e.g.*, the cardinality

of clusters) to detect a premature partition, these iCVIs were unable to patently identify over-partition solely based on the transitions of their values versus the number of clusters.

Moreover, although there is a natural order for the presentation of clusters (*i.e.*, as a time series), the presentation of samples within each cluster is random. Specifically, when the cluster is over-partitioned, samples are not presented in a subcluster-by-subcluster manner, but instead they are randomly sampled from the different subclusters. This adds another layer of complexity and thus makes this problem even more challenging. Compared to the correct partition in Fig. 4a, most iCVIs do not exhibit an overall behavior that deviates significantly from the one typically expected when accurately partitioning $D4$ (Fig. 4a), although most of them yield worse cluster quality evaluation values. In reality, in a true unsupervised learning scenario, such reference behavior is unavailable; furthermore, the values of most iCVIs are not bounded, thus making this problem even more challenging to detect.

Except for the `iConn_Index`, none of the iCVIs provided distinctive insights on the over-partition problem: there is a noticeable decrease of `iConn_Index` values (due to a large increase of `Inter_Conn` and decrease of `Intra_Conn`), especially considering that this iCVI's value is bounded to the interval $[0, 1]$. More importantly, following the over-partition, it does not exhibit the general behavior previously observed in Figs. 2c and 4c, and it maintains its poor assessment of the clustering solution, thus indicating that there is an issue with the partition found by the clustering algorithm.

VI. INCREMENTAL VERSUS BATCH IMPLEMENTATIONS

When evaluated over time, most iCVIs discussed in this study yield the same values as their batch counterparts (*e.g.*, the the recursive formulation of compactness is an exact computation, not an approximation [12], [13]). The only exception is the `iConn_Index`, which is the subject of analysis of this section. Figs. 6 to 9 illustrate the evolution of both `Conn_Index` and `iConn_Index` for all four experiments described in Section V. These figures also show the error (difference) between the batch and incremental implementations of the `Conn_Index` after the presentation of each sample. To obtain the batch `Conn_Index` values, fuzzy SMART was set to evaluation mode and all first and second winning prototypes were recomputed after the presentation of each sample.

Notably, error spikes consistently occur on the appearance of new clusters. In general, the error gradually diminishes over time, as samples within a given cluster are continuously presented to

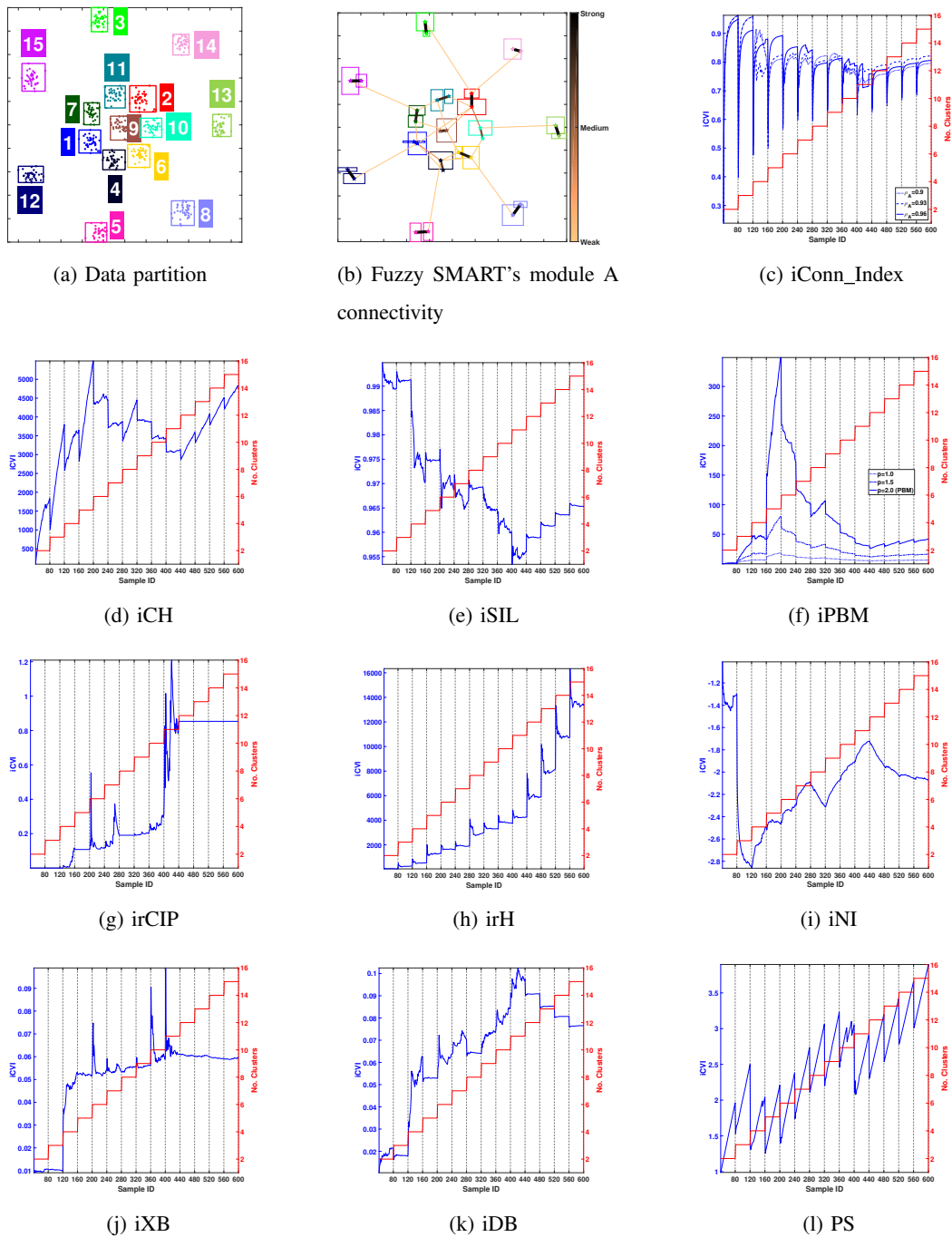


Fig. 2. (a) A high-quality partition of the data set *R15* by fuzzy ART-based clustering algorithms ($ARI = 0.9821$, $\rho = 0.88$). (b) Fuzzy SMART's module A categories ($\rho_A = 0.9$) and CONNvis [55] (thicker and darker lines indicate stronger connections). (c)-(l) Behavior of the iCVIs (blue curve) for the partition in (a). The number of clusters is tracked by the step-like red curve. The dashed vertical lines represent the limits between two consecutive clusters (ground truth), *i.e.*, samples before a line belong to one cluster whereas samples after it belong to another.

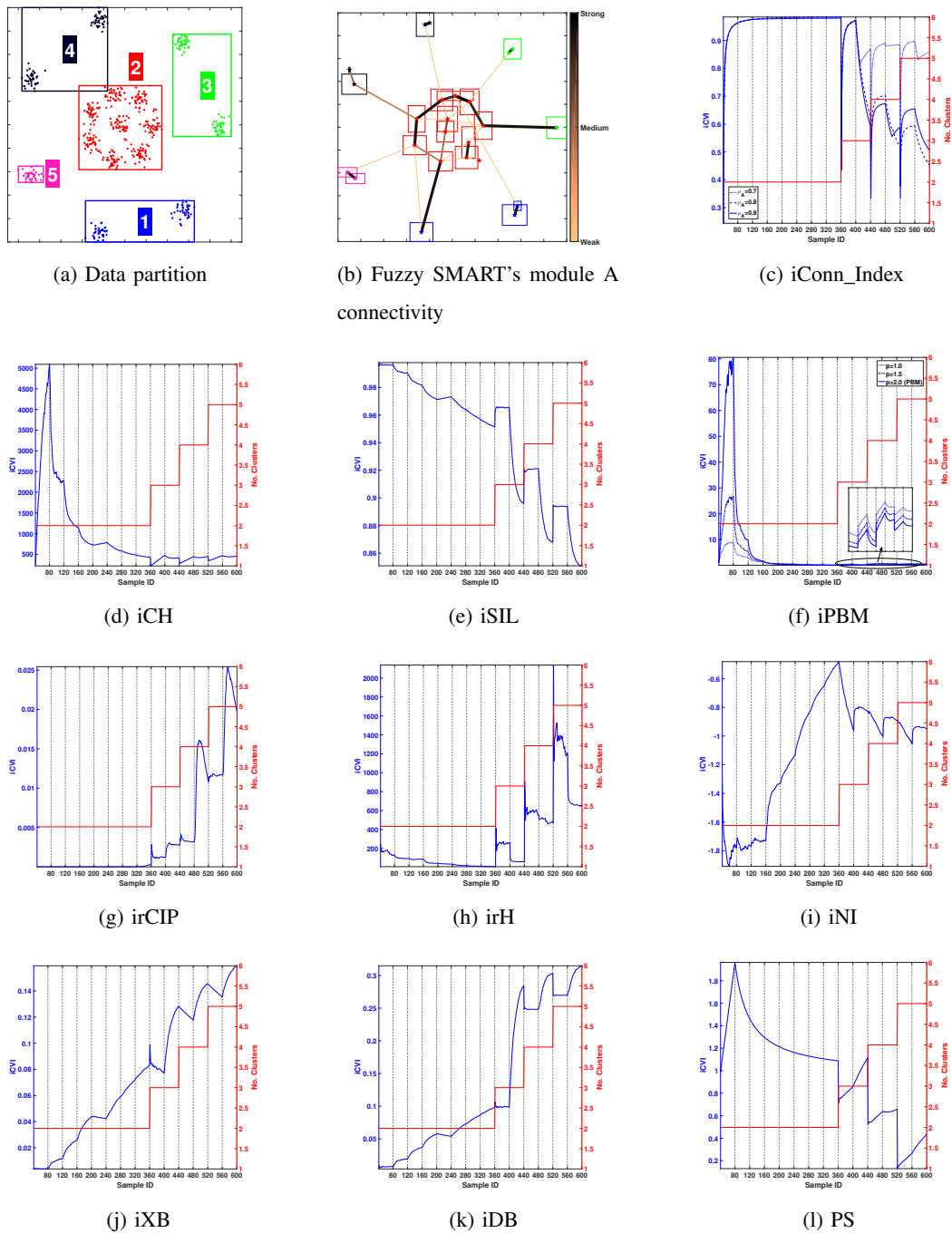


Fig. 3. (a) An under-partition of the data set *R15* by fuzzy ART-based clustering algorithms ($ARI = 0.2371$, $\rho = 0.61$). (b) Fuzzy SMART's module A categories ($\rho_A = 0.9$) and CONNvis [55] (thicker and darker lines indicate stronger connections). (c)-(l) Behavior of the iCVIs (blue curve) for the partition in (a). The number of clusters is tracked by the step-like red curve. The dashed vertical lines represent the limits between two consecutive clusters (ground truth), *i.e.*, samples before a line belong to one cluster whereas samples after it belong to another.

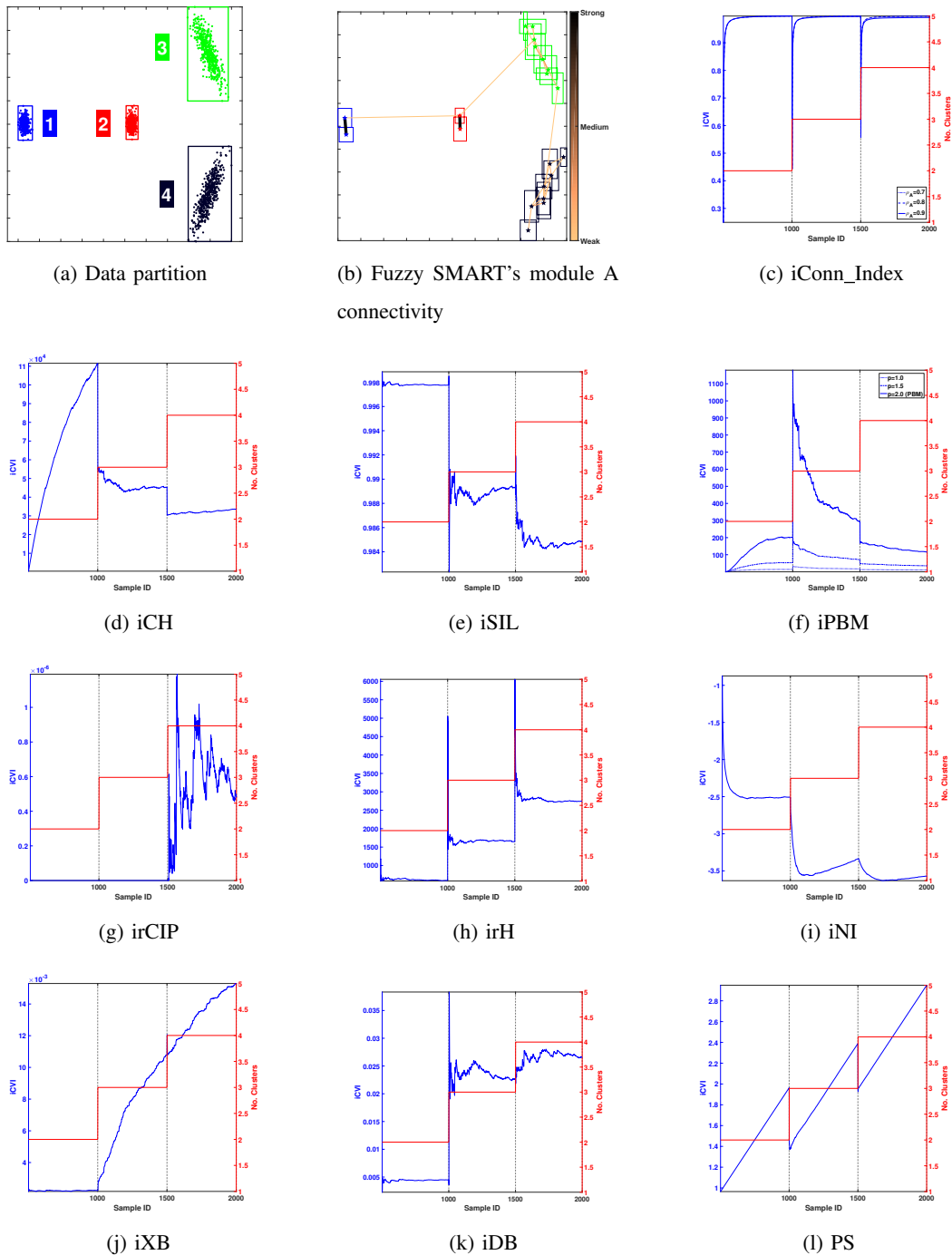


Fig. 4. (a) A high-quality partitioning of the *D4* data set by fuzzy ART-based clustering algorithms ($ARI = 1.0$, $\rho = 0.69$). (b) Fuzzy SMART's module A categories ($\rho_A = 0.9$) and CONNvis [55] (thicker and darker lines indicate stronger connections). (c)-(l) Behavior of the iCVIs (blue curve) for the partition in (a). The number of clusters is tracked by the step-like red curve. The dashed vertical lines represent the limits between two consecutive clusters (ground truth), *i.e.*, samples before a line belong to one cluster whereas samples after it belong to another.

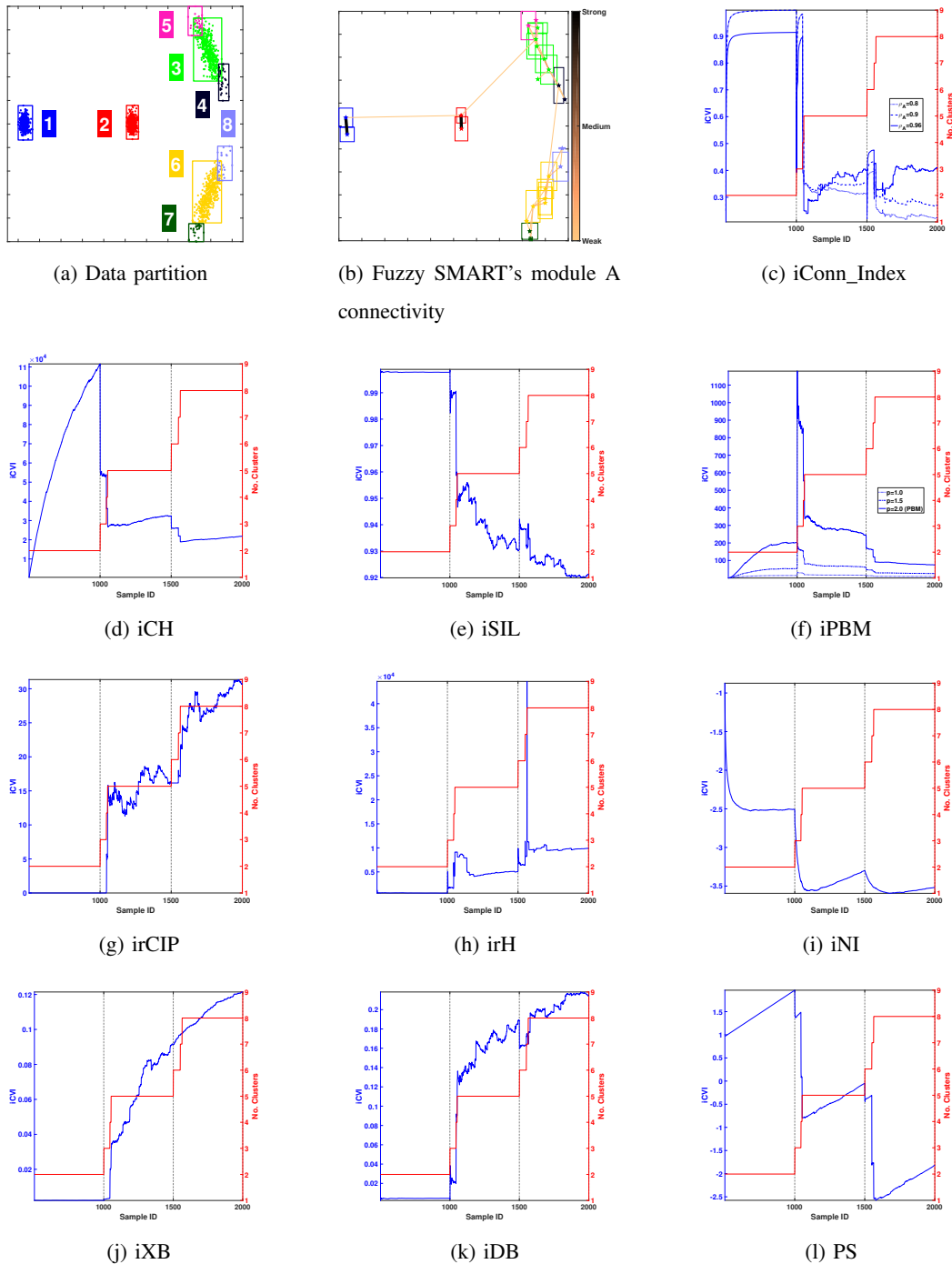
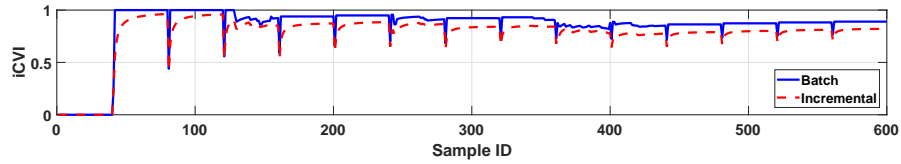
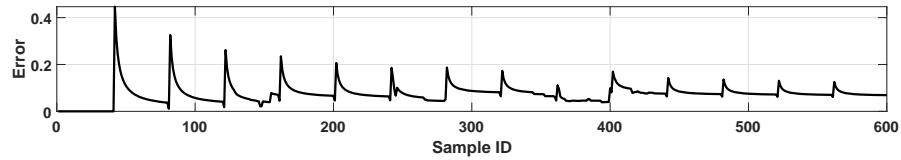


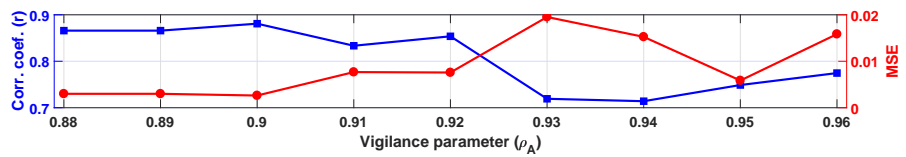
Fig. 5. (a) An over-partition of the $D4$ data set by fuzzy ART-based clustering algorithms ($ARI = 0.9315$, $\rho = 0.80$). (b) Fuzzy SMART's module A categories ($\rho_A = 0.9$) and CONNvis [55] (thicker and darker lines indicate stronger connections). (c)-(l) Behavior of the iCVIs (blue curve) for the partition in (a). The number of clusters is tracked by the step-like red curve. The dashed vertical lines represent the limits between two consecutive clusters (ground truth), *i.e.*, samples before a line belong to one cluster whereas samples after it belong to another.



(a) Conn_Index and iConn_Index behaviors ($\rho_A = 0.92$)

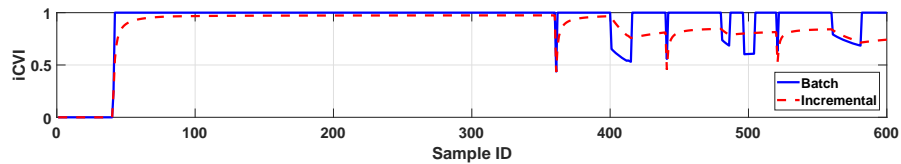


(b) $Error = Conn_Index - iConn_Index$

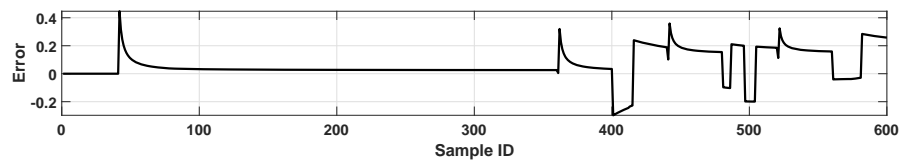


(c) Correlation coefficient and MSE

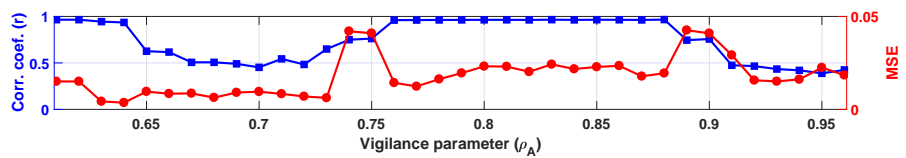
Fig. 6. (a) Behaviors of Conn_Index (continuous blue line) and iConn_Index (dashed red line) for the high-quality partitioning of the *R15* data set (Fig. 2). (b) Error between the batch and incremental versions in (a). (c) Correlation coefficients and MSE between the batch and incremental versions for fuzzy SMART’s module A vigilance parameter $\rho_A \in [\rho_B, 0.96]$.



(a) Conn_Index and iConn_Index behaviors ($\rho_A = 0.92$)

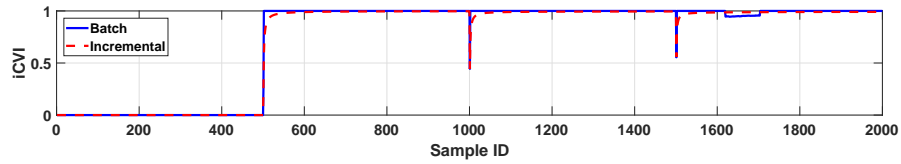


(b) $Error = Conn_Index - iConn_Index$

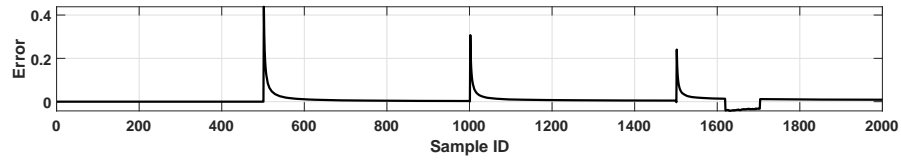


(c) Correlation coefficient and MSE

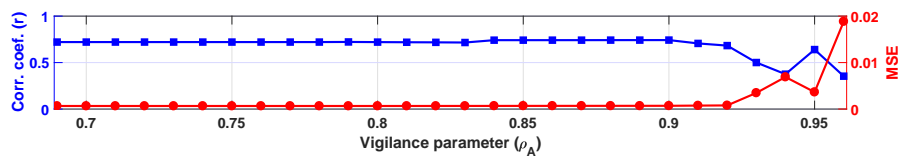
Fig. 7. (a) Behaviors of Conn_Index (continuous blue line) and iConn_Index (dashed red line) for the under-partitioning of the *R15* data set (Fig. 3). (b) Error between the batch and incremental versions in (a). (c) Correlation coefficients and MSE between the batch and incremental versions for fuzzy SMART’s module A vigilance parameter $\rho_A \in [\rho_B, 0.96]$.



(a) Conn_Index and iConn_Index behaviors ($\rho_A = 0.92$)

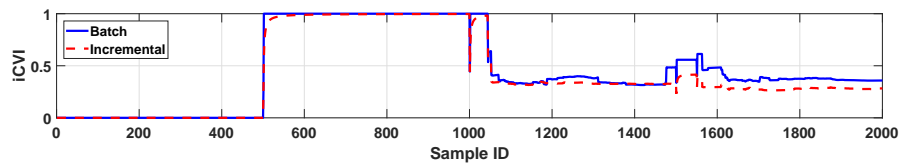


(b) $Error = Conn_Index - iConn_Index$

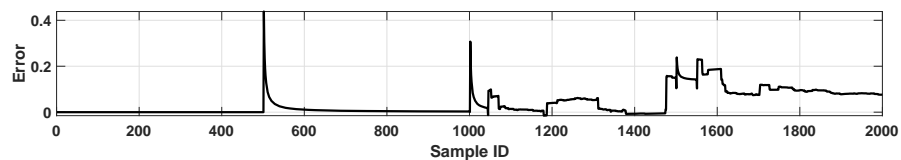


(c) Correlation coefficient and MSE

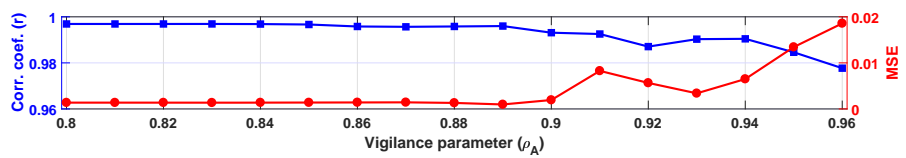
Fig. 8. (a) Behaviors of Conn_Index (continuous blue line) and iConn_Index (dashed red line) for the high-quality partitioning of the $D4$ data set (Fig. 4). (b) Error between the batch and incremental versions in (a). (c) Correlation coefficients and MSE between the batch and incremental versions for fuzzy SMART’s module A vigilance parameter $\rho_A \in [\rho_B, 0.96]$.



(a) Conn_Index and iConn_Index behaviors ($\rho_A = 0.92$)



(b) $Error = Conn_Index - iConn_Index$



(c) Correlation coefficient and MSE

Fig. 9. (a) Behaviors of Conn_Index (continuous blue line) and iConn_Index (dashed red line) for the over-partitioning of the $D4$ data set (Fig. 5). (b) Error between the batch and incremental versions in (a). (c) Correlation coefficients and MSE between the batch and incremental versions for fuzzy SMART’s module A vigilance parameter $\rho_A \in [\rho_B, 0.96]$.

the system. These trends are particularly clear when fuzzy SMART yield high quality partitions (Figs. 6 and 8). Regarding the cases of under- and over-partitioning (Figs. 7 and 9), the errors are more pronounced. However, iConn_Index still smoothly follows the overall trends of its batch counterpart (which has a more jagged behavior).

Finally, the effect of fuzzy SMART module A's quantization level on the similarity of the batch and incremental implementations was investigated. This was done by varying its vigilance parameter ρ_A in the closed interval $[\rho_B, 0.96]$ (larger values of ρ_A produce finer granularity of cluster prototypes). The Pearson correlation coefficients [80] and the mean squared error (MSE) depicted in Figs. 6c, 7c, 8c, and 9c show that the behavior of iConn_Index is consistent with Conn_Index across wide ranges of fuzzy SMART module A's vigilance. Interestingly, their dissimilarity tends to increase with very large vigilance values. These results support the original assumption, stated in Section III-F, that both versions of the Conn_Index would behave similarly. Therefore, iConn_Index is suitable for monitoring the performance online clustering methods.

VII. CONCLUSION

This paper extended six cluster validity indices (CVIs) to incremental versions, namely, incremental Calinski-Harabasz (iCH), incremental I index and incremental Pakhira-Bandyopadhyay-Maulik (iI and iPBM), incremental Silhouette (iSIL), incremental Negentropy Increment (iNI), incremental Representative Cross Information Potential (irCIP) and Cross Entropy (irH), and incremental Conn_Index (iConn_Index). Furthermore, using fuzzy adaptive resonance theory (ART)-based clustering algorithms, three different scenarios were analyzed: detection of the correct number of clusters in high-quality partitions, under- and over-partitioning. In such scenarios, a comparative study was performed among the presented incremental cluster validity indices (iCVIs), the Partition Separation (PS) index, the incremental Xie-Beni (iXB), and the incremental Davies-Bouldin (iDB).

As expected from previous studies, most iCVIs undergo abrupt changes following the creation of a new cluster. When samples from the same cluster are presented, however, each iCVI exhibits a particular behavior, which was taken as a reference to compare the cases of under- and over-partitioning a data set. In these experiments, the least visually informative iCVIs (*i.e.*, that provided less useful visual cues/hints in their behavior) were irCIP and iXB. Particularly, most iCVIs detected under-partitioning in at least one stage of the incremental clustering process, whereas only the iConn_Index provided some insight to indicate over-partitioning problems.

Nonetheless, the `iConn_Index` failed in identifying one of the under-partitioning cases. Therefore, the usual recommendation regarding batch CVIs also applies to iCVIs: this research highlights the importance of monitoring a number of iCVI dynamics at any given time, rather than relying on the assessment of only one. Finally, it was shown that, although not equal to its batch counterpart, the `iConn_Index` follows the same general trends. It is expected that the observations from the study presented here will assist in incremental clustering applications such as data streams.

ACKNOWLEDGMENT

This research was sponsored by the Missouri University of Science and Technology Mary K. Finley Endowment and Intelligent Systems Center; the Coordenação de Aperfeiçoamento de Pessoal de Nível Superior - Brazil (CAPES) - Finance code BEX 13494/13-9; the U.S. Dept. of Education Graduate Assistance in Areas of National Need program; and the Army Research Laboratory (ARL), and it was accomplished under Cooperative Agreement Number W911NF-18-2-0260. The views and conclusions contained in this document are those of the authors and should not be interpreted as representing the official policies, either expressed or implied, of the Army Research Laboratory or the U.S. Government. The U.S. Government is authorized to reproduce and distribute reprints for Government purposes notwithstanding any copyright notation herein. The authors would also like to thank Prof. James M. Keller and his coauthors for providing an early copy of reference [15].

REFERENCES

- [1] A. D. Gordon, "Cluster Validation," in *Data Science, Classification, and Related Methods*, C. Hayashi, K. Yajima, H.-H. Bock *et al.*, Eds. Tokyo: Springer Japan, 1998, pp. 22–39.
- [2] R. Xu, J. Xu, and D. C. Wunsch II, "A Comparison Study of Validity Indices on Swarm-Intelligence-Based Clustering," *IEEE Trans. Syst., Man, Cybern. B*, vol. 42, no. 4, pp. 1243–1256, Aug 2012.
- [3] L. E. Brito da Silva and D. C. Wunsch II, "A study on exploiting VAT to mitigate ordering effects in Fuzzy ART," in *Proc. Int. Joint Conf. Neural Netw. (IJCNN)*, 2018, pp. 2351–2358.
- [4] G. W. Milligan and M. C. Cooper, "An examination of procedures for determining the number of clusters in a data set," *Psychometrika*, vol. 50, no. 2, pp. 159–179, Jun 1985.
- [5] J. C. Bezdek, W. Q. Li, Y. Attikiouzel *et al.*, "A geometric approach to cluster validity for normal mixtures," *Soft Computing*, vol. 1, no. 4, pp. 166–179, Dec 1997.
- [6] M. Halkidi, Y. Batistakis, and M. Vazirgiannis, "Cluster Validity Methods: Part I," *SIGMOD Rec.*, vol. 31, no. 2, pp. 40–45, Jun. 2002.
- [7] M. Halkidi, Y. Batistakis, and M. Vazirgiannis, "Clustering Validity Checking Methods: Part II," *SIGMOD Rec.*, vol. 31, no. 3, pp. 19–27, Sep. 2002.

- [8] L. Vendramin, R. J. G. B. Campello, and E. R. Hruschka, "Relative clustering validity criteria: A comparative overview," *Statistical Analysis and Data Mining*, vol. 3, no. 4, pp. 209–235, 2010.
- [9] O. Arbelaitz, I. Gurrutxaga, J. Muguerza *et al.*, "An extensive comparative study of cluster validity indices," *Pattern Recognit.*, vol. 46, no. 1, pp. 243 – 256, 2013.
- [10] R. Xu and D. C. Wunsch II, "Survey of clustering algorithms," *IEEE Trans. Neural Netw.*, vol. 16, no. 3, pp. 645–678, May 2005.
- [11] R. Xu and D. C. Wunsch II, *Clustering*. Wiley-IEEE Press, 2009.
- [12] M. Moshtaghi, J. C. Bezdek, S. M. Erfani *et al.*, "Online Cluster Validity Indices for Streaming Data," *ArXiv e-prints*, Jan 2018, arXiv:1801.02937v1 [stat.ML].
- [13] M. Moshtaghi, J. C. Bezdek, S. M. Erfani *et al.*, "Online cluster validity indices for performance monitoring of streaming data clustering," *International Journal of Intelligent Systems*, vol. 0, no. 0, pp. 1–23, Nov 2018.
- [14] O. A. Ibrahim, J. M. Keller, and J. C. Bezdek, "Analysis of streaming clustering using an incremental validity index," in *2018 IEEE International Conference on Fuzzy Systems (FUZZ-IEEE)*, July 2018, pp. 1–8.
- [15] O. Ibrahim, Y. Wang, and J. Keller, "Analysis of incremental cluster validity for big data applications," *International Journal of Uncertainty, Fuzziness and Knowledge-Based Systems*, vol. 0, no. ja, p. null, 0.
- [16] O. Ibrahim, J. Keller, and J. Bezdek, "Evaluating Evolving Structure in Streaming Data with Modified Dunn's Indices," submitted to *IEEE Transaction on Evolving Topics in Computational Intelligence*, 2018.
- [17] G. A. Carpenter, S. Grossberg, and D. B. Rosen, "Fuzzy ART: Fast stable learning and categorization of analog patterns by an adaptive resonance system," *Neural Netw.*, vol. 4, no. 6, pp. 759 – 771, 1991.
- [18] G. Bartfai, "Hierarchical clustering with ART neural networks," in *Proc. Int. Conf. Neural Netw. (ICNN)*, vol. 2, Jun 1994, pp. 940–944.
- [19] D. Wunsch II, "ART properties of interest in engineering applications," in *Proc. Int. Joint Conf. Neural Netw. (IJCNN)*, Jun 2009, pp. 3380–3383.
- [20] T. Caliński and J. Harabasz, "A dendrite method for cluster analysis," *Communications in Statistics*, vol. 3, no. 1, pp. 1–27, 1974.
- [21] D. L. Davies and D. W. Bouldin, "A cluster separation measure," *IEEE Trans. Pattern Anal. Mach. Intell.*, vol. PAMI-1, no. 2, pp. 224–227, Apr 1979.
- [22] X. L. Xie and G. Beni, "A Validity Measure for Fuzzy Clustering," *IEEE Trans. Pattern Anal. Mach. Intell.*, vol. 13, no. 8, pp. 841–847, Aug 1991.
- [23] J. Lamirel and P. Cuxac, "New quality indexes for optimal clustering model identification with high dimensional data," in *2015 IEEE International Conference on Data Mining Workshop (ICDMW)*, Nov 2015, pp. 855–862.
- [24] J. Lamirel, N. Dugu, and P. Cuxac, "New efficient clustering quality indexes," in *Proc. Int. Joint Conf. Neural Netw. (IJCNN)*, July 2016, pp. 3649–3657.
- [25] S. Bandyopadhyay and U. Maulik, "Nonparametric genetic clustering: comparison of validity indices," *IEEE Trans. Syst., Man, Cybern. C*, vol. 31, no. 1, pp. 120–125, Feb 2001.
- [26] M. K. Pakhira, S. Bandyopadhyay, and U. Maulik, "Validity index for crisp and fuzzy clusters," *Pattern Recognit.*, vol. 37, no. 3, pp. 487 – 501, 2004.
- [27] P. J. Rousseeuw, "Silhouettes: A graphical aid to the interpretation and validation of cluster analysis," *Journal of Computational and Applied Mathematics*, vol. 20, pp. 53 – 65, 1987.
- [28] E. R. Hruschka, L. N. de Castro, and R. J. G. B. Campello, "Evolutionary algorithms for clustering gene-expression data," in *Proc. IEEE Int. Conf. Data Mining (ICDM)*, Nov 2004, pp. 403–406.

- [29] E. R. Hruschka, R. J. Campello, and L. N. de Castro, “Evolving clusters in gene-expression data,” *Information Sciences*, vol. 176, no. 13, pp. 1898 – 1927, 2006.
- [30] M. Rawashdeh and A. Ralescu, “Center-wise intra-inter silhouettes,” in *Scalable Uncertainty Management*, E. Hüllermeier, S. Link, T. Fober *et al.*, Eds. Berlin, Heidelberg: Springer, 2012, pp. 406–419.
- [31] J. M. Luna-Romera, M. del Mar Martínez-Ballesteros, J. García-Gutiérrez *et al.*, “An Approach to Silhouette and Dunn Clustering Indices Applied to Big Data in Spark,” in *Advances in Artificial Intelligence*, O. Luaces, J. A. Gámez, E. Barrenechea *et al.*, Eds. Cham: Springer International Publishing, 2016, pp. 160–169.
- [32] J. d. A. Silva and E. R. Hruschka, “A support system for clustering data streams with a variable number of clusters,” *ACM Trans. Auton. Adapt. Syst.*, vol. 11, no. 2, pp. 11:1–11:26, Jul. 2016.
- [33] M.-S. Yang and K.-L. Wu, “A new validity index for fuzzy clustering,” in *10th IEEE International Conference on Fuzzy Systems. (Cat. No.01CH37297)*, vol. 1, Dec 2001, pp. 89–92.
- [34] E. Lughofer, “Extensions of vector quantization for incremental clustering,” *Pattern Recognit.*, vol. 41, no. 3, pp. 995 – 1011, 2008, part Special issue: Feature Generation and Machine Learning for Robust Multimodal Biometrics.
- [35] L. F. Lago-Fernández and F. Corbacho, “Normality-based validation for crisp clustering,” *Pattern Recognit.*, vol. 43, no. 3, pp. 782 – 795, 2010.
- [36] L. F. Lago-Fernández and F. Corbacho, “Using the negentropy increment to determine the number of clusters,” in *Bio-Inspired Systems: Computational and Ambient Intelligence: 10th International Work-Conference on Artificial Neural Networks*, J. Cabestany, F. Sandoval, A. Prieto *et al.*, Eds. Berlin, Heidelberg: Springer, 2009, pp. 448–455.
- [37] P. Comon, “Independent component analysis, A new concept?” *Signal Processing*, vol. 36, no. 3, pp. 287 – 314, 1994.
- [38] D. Araújo, A. D. Neto, and A. Martins, “Representative cross information potential clustering,” *Pattern Recognit. Lett.*, vol. 34, no. 16, pp. 2181 – 2191, 2013.
- [39] D. Araújo, A. D. Neto, and A. Martins, “Information-theoretic clustering: A representative and evolutionary approach,” *Expert Syst. Appl.*, vol. 40, no. 10, pp. 4190 – 4205, 2013.
- [40] E. Gokcay and J. C. Principe, “A new clustering evaluation function using Renyi’s information potential,” in *Proc. Int. Conf. Acoust., Speech, Signal Process. (ICASSP)*, vol. 6, 2000, pp. 3490–3493.
- [41] E. Gokcay and J. C. Principe, “Information theoretic clustering,” *IEEE Trans. Pattern Anal. Mach. Intell.*, vol. 24, no. 2, pp. 158–171, Feb. 2002.
- [42] A. Rényi, “On Measures of Entropy and Information,” in *Proc. 4th Berkeley Symp. Math. Statist. Probab., Contrib. Theory Statist.*, vol. 1. Berkeley, CA: University of California Press, 1961, pp. 547–561.
- [43] R. O. Duda, P. E. Hart, and D. G. Stork, *Pattern Classification*, 2nd ed. John Wiley & Sons, 2000.
- [44] M. Cottrell and P. Rousset, “The kohonen algorithm: A powerful tool for analysing and representing multidimensional quantitative and qualitative data,” in *Biological and Artificial Computation: From Neuroscience to Technology*, J. Mira, R. Moreno-Díaz, and J. Cabestany, Eds. Berlin, Heidelberg: Springer Berlin Heidelberg, 1997, pp. 861–871.
- [45] G. Karypis, E.-H. Han, and V. Kumar, “Chameleon: hierarchical clustering using dynamic modeling,” *Computer*, vol. 32, no. 8, pp. 68–75, Aug 1999.
- [46] E. W. Tyree and J. Long, “The use of linked line segments for cluster representation and data reduction,” *Pattern Recognit. Lett.*, vol. 20, no. 1, pp. 21 – 29, 1999.
- [47] J. Vesanto and E. Alhoniemi, “Clustering of the self-organizing map,” *IEEE Trans. Neural Netw.*, vol. 11, no. 3, pp. 586–600, May 2000.
- [48] L. N. F. Ana and A. K. Jain, “Robust data clustering,” in *2003 IEEE Computer Society Conference on Computer Vision and Pattern Recognition, 2003. Proceedings.*, vol. 2, June 2003, pp. II–II.

- [49] J. C. Principe, *Information Theoretic Learning: Renyi's Entropy and Kernel Perspectives*, 1st ed. Springer Publishing Company, Incorporated, 2010.
- [50] A. G. Oliveira, A. D. Neto, and A. Martins, "An analysis of information dynamic behavior using autoregressive models," *Entropy*, vol. 19, no. 11, 2017.
- [51] A. G. Oliveira, A. Martins, and A. D. Neto, "Information state: A representation for dynamic processes using information theory," in *Proc. Int. Joint Conf. Neural Netw. (IJCNN)*, July 2018, pp. 1–8.
- [52] K. Taşdemir and E. Merényi, "A new cluster validity index for prototype based clustering algorithms based on inter- and intra-cluster density," in *Proc. Int. Joint Conf. Neural Netw. (IJCNN)*, Aug. 2007, pp. 2205–2211.
- [53] K. Taşdemir and E. Merényi, "A Validity Index for Prototype-Based Clustering of Data Sets With Complex Cluster Structures," *IEEE Trans. Syst., Man, Cybern. B*, vol. 41, no. 4, pp. 1039–1053, Aug. 2011.
- [54] K. Taşdemir and E. Merényi, "Data topology visualization for the Self-Organizing Maps," in *Proc. 14th European Symposium on Artificial Neural Networks (ESANN 2006)*, Apr. 2006, pp. 277–282.
- [55] K. Taşdemir and E. Merényi, "Exploiting Data Topology in Visualization and Clustering of Self-Organizing Maps," *IEEE Trans. Neural Netw.*, vol. 20, no. 4, pp. 549–562, Apr. 2009.
- [56] S. Araki, H. Nomura, and N. Wakami, "Segmentation of thermal images using the fuzzy c-means algorithm," in *Proc. Second IEEE International Conference on Fuzzy Systems*, vol. 2, Mar 1993, pp. 719–724.
- [57] G. A. Carpenter and S. Grossberg, "A massively parallel architecture for a self-organizing neural pattern recognition machine," *Computer Vision, Graphics, and Image Processing*, vol. 37, no. 1, pp. 54 – 115, 1987.
- [58] G. A. Carpenter and S. Grossberg, "ART 2: self-organization of stable category recognition codes for analog input patterns," *Appl. Opt.*, vol. 26, no. 23, pp. 4919–4930, Dec 1987.
- [59] G. A. Carpenter and S. Grossberg, "The ART of adaptive pattern recognition by a self-organizing neural network," *Computer*, vol. 21, no. 3, pp. 77–88, March 1988.
- [60] G. A. Carpenter and S. Grossberg, "ART 3: Hierarchical search using chemical transmitters in self-organizing pattern recognition architectures," *Neural Netw.*, vol. 3, no. 2, pp. 129–152, 1990.
- [61] R. Xu and D. C. Wunsch II, "BARTMAP: A viable structure for biclustering," *Neural Netw.*, vol. 24, no. 7, pp. 709–716, sep 2011.
- [62] L. E. Brito da Silva, I. Elnabarawy, and D. C. Wunsch II, "Dual vigilance fuzzy adaptive resonance theory," *Neural Netw.*, vol. 109, pp. 1–5, 2019.
- [63] L. E. Brito da Silva, I. Elnabarawy, and D. C. Wunsch II, "Distributed dual vigilance fuzzy adaptive resonance theory learns online, retrieves arbitrarily-shaped clusters, and mitigates order dependence," *arXiv e-prints*, Nov. 2018, arXiv:1901.00794[cs.NE].
- [64] P. P. Chen, W.-C. Lin, and H.-L. Hung, "Multi-resolution fuzzy ART neural networks," in *Proc. Int. Joint Conf. Neural Netw. (IJCNN)*, vol. 3, 1999, pp. 1973–1978.
- [65] J. R. Williamson, "Gaussian ARTMAP: A Neural Network for Fast Incremental Learning of Noisy Multidimensional Maps," *Neural Netw.*, vol. 9, no. 5, pp. 881 – 897, 1996.
- [66] G. Anagnostopoulos and M. Georgiopoulos, "Hypersphere ART and ARTMAP for unsupervised and supervised, incremental learning," in *Proc. Int. Joint Conf. Neural Netw. (IJCNN)*, vol. 6, 2000, pp. 59–64 vol.6.
- [67] G. Anagnostopoulos and M. Georgiopoulos, "Ellipsoid ART and ARTMAP for incremental clustering and classification," in *Proc. Int. Joint Conf. Neural Netw. (IJCNN)*, vol. 2, 2001, pp. 1221–1226 vol.2.
- [68] B. Vigdor and B. Lerner, "The Bayesian ARTMAP," *IEEE Trans. Neural Netw.*, vol. 18, no. 6, pp. 1628–1644, 2007.
- [69] N. Brannon, G. Conrad, T. Draelos *et al.*, "Information fusion and situation awareness using artmap and partially observable markov decision processes," in *Proc. Int. Joint Conf. Neural Netw. (IJCNN)*, 2006, pp. 2023–2030.

- [70] Y.-T. Huang, F.-T. Cheng, Y.-H. Shih *et al.*, “Advanced ART2 scheme for enhancing metrology-data-quality evaluation,” *Journal of the Chinese Institute of Engineers*, vol. 37, no. 8, pp. 1064–1079, 2014.
- [71] H. Isawa, H. Matsushita, and Y. Nishio, “Fuzzy Adaptive Resonance Theory Combining Overlapped Category in consideration of connections,” in *Proc. Int. Joint Conf. Neural Netw. (IJCNN)*, June 2008, pp. 3595–3600.
- [72] L. E. Brito da Silva and D. C. Wunsch II, “Validity index-based vigilance test in adaptive resonance theory neural networks,” in *2017 IEEE Symposium Series on Computational Intelligence (SSCI)*, Nov. 2017, pp. 1–8.
- [73] L. A. Zadeh, “Fuzzy sets,” *Information and Control*, vol. 8, no. 3, pp. 338 – 353, 1965.
- [74] L. E. Brito da Silva and D. C. Wunsch II, “An Information-Theoretic-Cluster Visualization for Self-Organizing Maps,” *IEEE Trans. Neural Netw. Learn. Syst.*, vol. 29, no. 6, pp. 2595–2613, June 2018.
- [75] G. A. Carpenter and N. Markuzon, “Artmap-ic and medical diagnosis: Instance counting and inconsistent cases,” *Neural Netw.*, vol. 11, no. 2, pp. 323 – 336, 1998.
- [76] K. Wang, B. Wang, and L. Peng, “CVAP: Validation for Cluster Analyses,” *Data Science Journal*, vol. 8, pp. 88–93, 2009.
- [77] L. Hubert and P. Arabie, “Comparing partitions,” *J. Classification*, vol. 2, no. 1, pp. 193–218, 1985.
- [78] C. J. Veenman, M. J. T. Reinders, and E. Backer, “A maximum variance cluster algorithm,” *IEEE Trans. Pattern Anal. Mach. Intell.*, vol. 24, no. 9, pp. 1273–1280, Sept. 2002.
- [79] Pasi Fränti *et al.*, “Clustering datasets,” 2015, accessed on May 4, 2017. [Online]. Available: <http://cs.uef.fi/sipu/datasets/>
- [80] L. J. Bain and M. Engelhardt, *Introduction to Probability and Mathematical Statistics*, 2nd ed. Brooks/Cole, Cengage Learning, 1992.